Available online www.ejaet.com

European Journal of Advances in Engineering and Technology, 2018, 5(11): 879-887

Research Article ISSN: 2394 - 658X

Testing of High Speed Data Transmission over a Fading Channel on a Graphics Processing Unit for Software Defined Radio

Rehan Muzammil

Department of Electronics Engineering Aligarh Muslim University,
Aligarh, India-202002
rehan_muzammil@rediffmail.com

ABSTRACT

5G mobile communication networks are emerging in order to cover the extreme needs for high data rates for delivering multimedia data to mobile communication users. High transmission bit rate in wireless channels gives rise to severe inter-symbol interference (ISI) and this makes the detection task very challenging. In such cases, Near-Maximum-Likelihood (NML) detection gives good performance. This paper describes the Testing of a High Speed Multi-Level data transmission system using NML detection on a Graphics Processing Unit (GPU) using CUDA-C++ programming language. The GPU over which the system is tested is NVIDIA GeForce GTX 1050 Ti. The system program is run on a Core-i3 8th generation CPU and the processing time for the various parameters illustrated over the GPU. The simulation is performed for QAM-4 modulation scheme. The data is transmitted over a frequency selective fading channel with two independently Rayleigh fading paths at a frequency of 5 GHz (well suited for 5G mobile), thus introducing ISI, and the results obtained are compared for varying Signal to Noise Ratios (SNR) for different channel configurations. All the simulation tests are performed for a mobile velocity of 80 km/hour in an urban environment and varying bit rates from 2 Mbps to 50 Mbps.

Key words: NMLD, ISI, GPU, QAM-4, 5G

INTRODUCTION

Software Defined Radio (SDR) is very high re-configurable hardware platform that provides the technology for realizing the rapidly growing technologies [9]. Many sophisticated signal-processing tasks are performed in the baseband section of the SDR. While there are an abundance of silicon alternatives available for implementation of various SDR baseband functions, Graphics Processing Units (GPUs) are an attractive for many of these tasks for reasons of performance, power consumption and configurability.SDR has the ability of changing the characteristics of a transmitting and receiving radio device without physically modifying the hardware [10].

Mobile communications provides connectivity that enables mobility and computing in many different communication environments. The huge demands for these systems are driving the growing development of mobile communications more rapidly than ever before. Because of this a large set of new advanced techniques have emerged brought forward by a larger bandwidth, more powerful processing capability, and advances in computing technology. Many new services are provided, or will be provided to potential users, and delivered with high quality by usage of GSM and wireless mesh networks in public, home, and corporate scenarios [1].

The high success of the mobile and multimedia communication services led to the advancement from 3G to 4G mobile communication systems, in order to increase the data rate to end users. The increase of traffic in the mobile Communications network due to the need of access to data communications anywhere and anytime and the growth of demand of high data rates drove the research to the development and design of next generation mobile communication systems, e.g. 5G systems.

Various mobile devices, wider transmission bandwidth, manifold wireless and wired networks, and more powerful appliances' processing capability, together with advances in computing technology have brought more and more miscellaneous services to be delivered with more excellent quality. Next generation mobile systems need the support of all the advances on new theories, algorithms, architectures, standards, and protocols. In the near future, more and more

Internet based services like web service can be smoothly accessed with various mobile devices through the wide deployed wireless networks [2].

In a society with advanced multimedia and ubiquitous communications services, computers and communication equipment will be all over the place, and communications will take place in all forms centering on mobile networks, not only between people, but also between a person and a machine (computer), and even between a machine and another machine. Under these circumstances, a huge increase in non-voice traffic will be expected in person-person, person-machine, and machine-machine communications [3]. The mobile communications system beyond IMT-2000 (4G) were designed to offer significantly higher bit rates than 2 Mb/s even in a vehicular environment and to adapt to data communications more efficiently to realize the concept of "anytime, anywhere, anyone, and anything" from the viewpoint of multimedia communications [4].

Considerable research into a next generation mobile communications system capable of achieving such wideband and high-speed data communications is currently under way. In order to realize such a high-speed data transmission system, it is necessary to prepare a wide frequency bandwidth. However, the frequencies around bands used for current mobile communications systems are already used in many other radio systems, and it is very difficult to newly secure a wide frequency band. For this reason, use of a high frequency band would be required for the next system. Moreover, improving the data transmission speed causes an increase in received signal power required by high speed transmission. These factors lead to reduce cell coverage area, which prompts need for many base stations in order to avoid dead spots [5].

In terms of the radio physical layer, it is seen that cellular radio link speed has increased from about 2 Mb/s with early 3G systems in the year 2000 to 100 Mb/s with 4G (LTE and WiMax) systems using multiple-input– multiple-output (MIMO) radio technology. Thus, wide-area cellular and short-range radio have become 30–50 times faster over this period, roughly matching Moore's law advances in computing speed. Clearly, we are currently in the midst of historic increases in wireless bit rate and system capacity to levels needed to support large-scale delivery of audiovisual and rich media applications [6].

Radio operation using QAM techniques working in SHF band with carrier frequency of 5 GHz (used in this work) provides reliable and consistent propagation within an urban environment. The 5GHz band, well suited for 5G network, also allows the use of economically priced highly efficient radio - frequency components with low power consumption resulting in good battery life. In a typical cellular mobile telephone system, the mobiles in a cell do not communicate directly with each other but only via the base station. The receiver here must carry out a process of estimation and detection on each individual received signal. These signals originate from different mobiles and occur in bursts. Thus, there is a continuous process involving the appearance of new signals and the disappearance of existing signals. Furthermore, different signals fade independently and may therefore have widely differing levels. Serious Doppler shifts may also be experienced [7].

A particular formidable problem in the transmission of the digital signals over a narrowband channel of land-mobile-radio system, operating in the 5 GHz band, is the rapid fading introduced into the signal by the channel. High transmission bit rate in wireless channels gives rise to severe Inter-Symbol Interference (ISI), and this makes the detection task extremely challenging. Hence in order to realize systems capable of working well even over such types of highly distortive channels, Near-Maximum-Likelihood (NML) detection techniques is used. It may also be mentioned here that previously the practical implementation of NML based systems was difficult due to its high computational complexity and large memory requirements [8].

The whole system is tested over a GPU. Programming GPUs remains a complicated task despite the recent advances made to make GPU programming simpler. More specifically the GPU is especially well suited to address problems that can be expressed as data-parallel computations – the same program is executed on many data elements in parallel. In the present paper, the author has described a practical implementation of NML detection technique in a QAM-4 transceiver, and this work deals with the design and testing of such a system on a GPU (NVIDIA GeForce GTX 1050 Ti) [8].

Section II describes the characteristics of fading channel. Section III illustrates the channel model for the multiple resolvable paths. Here in this paper the number of multiple resolvable paths taken is two. Section IV illustrates the Near-maximum-likelihood detection technique. Section V gives the design of the 5-Pole Bessel Filter used for channel generation. Section VI gives the Results and Discussions. Section VII draws the conclusions.

CHARACTERISTICS OF THE FADING CHANNEL

In a typical 5 GHz land mobile radio link, full duplex signals are passed between the vehicle on the move and the base station. The mobile is surrounded by tall buildings and other mobile units whereas the base station is mounted upon the nearby rooftop or any other convenient high point. The signal, due to this undergoes a multipath propagation due to reflections from the buildings and other mobile units. The radio waves travel at the speed of light. Different paths have different path lengths because of which there will be corresponding time difference in the arrival of the wave along each path. In addition, these paths are continuously changing due to the change in position of the mobile units i.e. at a speed related to the speed of the mobile, because of which the received signal undergoes rapid fading known as Rayleigh fading [7].

Due to multipath propagation in a channel, the transmission of a very narrow pulse results in the reception of a train of pulses. The time difference between reception of the first and the last of these pulses is known as the multipath delay spread of the channel. Multipath delay spread is a major limiting factor in the operation of the high-speed serial data transmission systems. When the multipath delay spread becomes large, the adjacent signal element may interfere with each other, causing inter-symbol interference (ISI), and thereby a degradation in the system performance. The ISI becomes serious when the multipath spread is approximately 40 % of the duration of the signal element. Multipath delay spread depends upon the frequency of transmission, type of environment, bandwidth of the system etc [7].

In most of the radio communication systems, there are often two or more different paths along which the radio signals travel from the transmitter antenna to the receiver antenna. However, the signal received on each path (often referred to as space wave in SHF transmission) is itself made up of slightly different paths, all adding randomly at the receiver. Each space wave could be thought of as the sum of number of vectors (phasors) having slightly different amplitudes and widely different phases. This gives rise to variation in the received signal, whichis referred to as fading. A fading channel consisting of a single space wave is very often referred to as Flat fading channel. The term "flat fading" is used to the fact that all the frequency components in the signal are affected in a similar manner. A frequency selective channel can be viewed as the one, which gives rise to two or more space waves at the receiver, where each has a different and resolvable multipath delay, and is affected differently by the channel. In frequency selective fading channels, different frequency components of the received signal may fade differently [7].

In the 5 GHz land mobile radio, a level of background noise w(t) is added to the information signal. This is almost equally composed of manmade noise from the vehicle ignition systems, and receiver front - end noise. The man made noise is generally described as Additive White Gaussian Noise (AWGN). Noise w(t) is modelled as stationary additive white GAUSSIAN noise with zero mean and variance equal to one [7].

CHANNEL MODEL FOR MULTIPLE RESOLVABLE PATHS

The performance of the mobile is determined more efficiently when the mobile is tested over a fading channel simulator using digital computer rather than direct on-the-air measurements. From the model based on the multipath propagation arising from multiple scattering of the radio waves by buildings and other structures in the vicinity of the mobile unit, it can be shown that the envelop of the received signal is Rayleigh distributed whereas the phase of the received signal is uniformly distributed between [0, 2π].

Fig. 1 illustrates the channel model where the input signal is fed to the tapped delay line. The delayed signal at each of the taps are modulated in amplitude as well as in phase by complex valued baseband random function in such a way that each of these represents a Rayleigh fading path. The number of taps is equal to the number of reflected signals reaching the receiver via different paths. Each tap gain function is independent of the other, which means that each of the reflected signals arrive via an independently fading path. The delayed and modulated signals are summed with additive noise which has a Gaussian probability density [7].

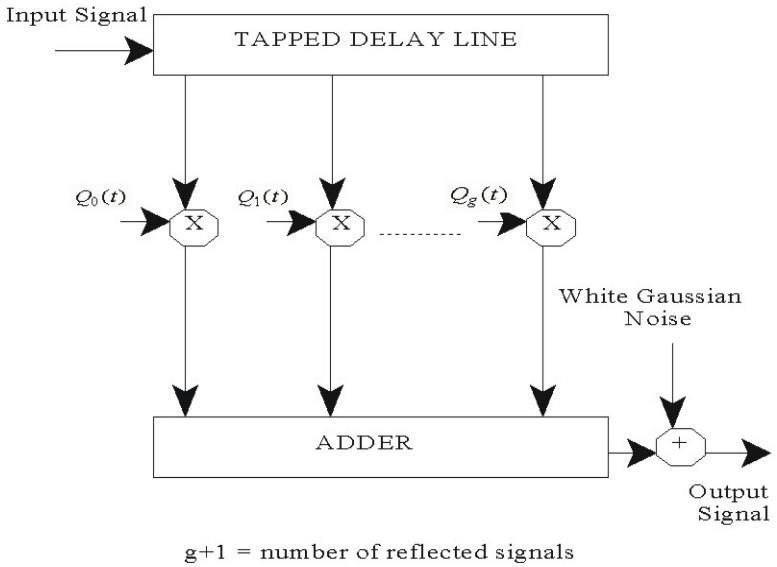

Fig. 1 Tapped Delay Line Model of the channel.

NEAR-MAXIMUM-LIKELIHOOD DETECTION TECHNIQUE

In this paper Near-maximum-likelihood, detection technique is used for QAM-4 modulation scheme [8]. Channel is the medium of propagation of the signal. At the receiver, AWGN is added to the signal. The channel, signal and noise are all considered complex with real and imaginary parts. The tapped delay line model of the channel is illustrated in Figure 1 and equation of received signal is given as Equation 1.

$$r_i = \sum_{h=0}^{g} s_{i-h}\, y_{i,h} + w_i \quad \ldots (1)$$

where, r_i, s_{i-h}, $y_{i,h}$, w_i are complex with real and imaginary parts which signifies In-phase (I) and Quadrature (Q) channels, (g+1) is the total number of independent fading paths, $y_{i,h}$ is Rayleigh fading channel component (of h^{th} fading path at i^{th} time instant), s_{i-h} is the present and the previously transmitted complex symbols, w_i is the complex Additive White Gaussian Noise (AWGN) component at i^{th} time instant.

The signal, channel and noise have uniform probability density function (pdf), Rayleigh pdf, and Gaussian pdf respectively. The algorithm for Near-Maximum-Likelihood Detection (NMLD) technique for QAM-4 is given as [8],Just prior to the receipt of the sample r_i(complex with real and imaginary parts), the detector has in store k different n-component vectors, $\{Q_{i-1}\}$ where,

$$Q_{i-1} = [x_{i-n} \quad x_{i-n+1} \quad x_{i-n+2} \quad x_{i-n+3} \dots \dots x_{i-1}] \quad \dots(2)$$

Moreover, x_{i-h}can take any of the four possible values for QAM-4 signal. Value of n is length of stored vectors and its value is chosen depending upon the number of components in the sampled impulse response of the channel.

Each $\{Q_{i-1}\}$ represents a possible sequence of data symbols

$$s_{i-n}, s_{i-n+1}, s_{i-n+2}, s_{i-n+3} \dots \dots \dots \dots s_{i-1} \quad \dots (3)$$

Also, each vector $\{Q_{i-1}\}$ is formed by last n components of the (i-1)-component vectorX_{i-1}, where

$$X_{i-1} = [x_1 x_2 x_3 x_4 \dots \dots \dots \dots \dots \dots \dots x_{i-1}] \quad \dots (4)$$

And has following associated cost:

$$U_{i-1} = \sum_{j=1}^{i-1} \left| r_j - \sum_{h=0}^{7} x_{j-h} y_{j,h} \right|^2 \quad \dots (5)$$

Where $y_{j,h}$ is the channel component and x_i=0 for i≤0

$U_{i-1}$is also taken to be the cost of the corresponding vector Q_{i-1}. Equation 5 is the generalized form for the cost U_{i-1}. It can be seen that the vector X_{i-1} most likely to be correct is that which has the smallest cost U_{i-1} over all combinations of the possible values of $\{x_j\}$. On the receipt of sampler_i, each of the k stored vectors $\{Q_{i-1}\}$ is expanded into m (n+1) - component vectors $\{P_i\}$ as shown in the Figure 2 where

$$P_i = [x_{i-n} x_{i-n+1} x_{i-n+2} \dots \dots \dots \dots \dots \dots x_i] \quad \dots (6)$$

Moreover, m is the number of possible values of vectors $\{P_i\}$, derived from any vector $\{Q_{i-1}\}$. The first n components are as in original $\{Q_{i-1}\}$ and the last component x_i takes on its four possible values of s_i. With each of the resulting vectors is associated its cost U_i given as:

$$U_i = U_{i-1} + \left| r_i - \sum_{h=0}^{7} x_{i-h} y_{i,h} \right|^2 \quad \dots (7)$$

Where U_{i-1} is the cost of the vector Q_{i-1} from which P_i is derived.

For a channel with a single fading path (or a flat fading channel), g=1. For an AWGN channel having no ISI and no fading, we may assume $y_{i,h}$=1 and Equation 7 can then be simplified as:

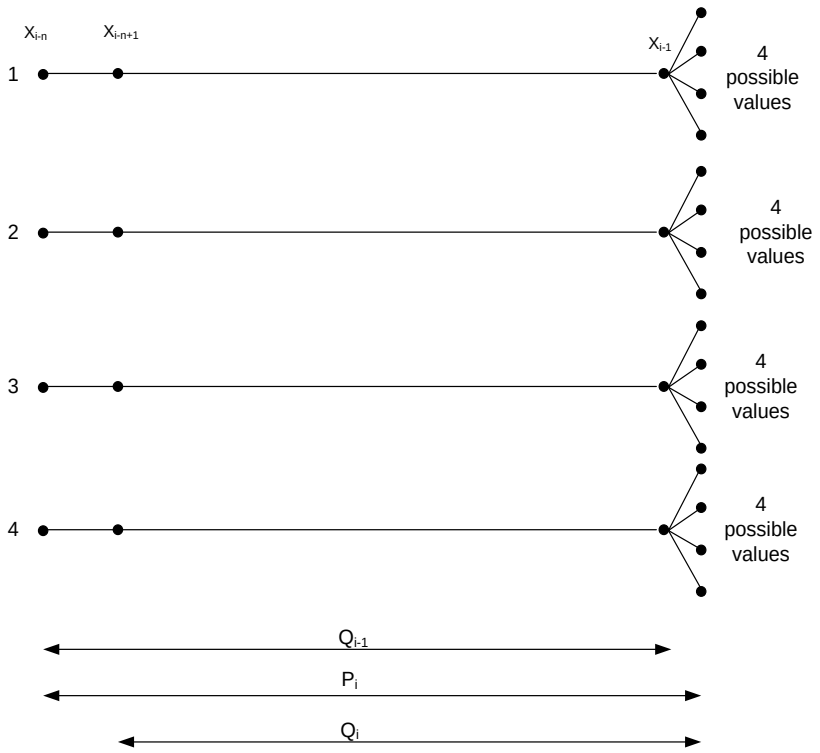

Fig. 2 Expansion of vectors $\{Q_{i-1}\}$ into $\{P_i\}$ for QAM-4

$$U_i = U_{i-1} + |r_i - x_i|^2 \quad \ldots (8)$$

Where r_i is the received signal and x_i is the possible value of the transmitted data symbol. The vector with the smallest cost U_i is selected from a resulting set of 4 x 4 expanded vectors $\{P_i\}$. The detected value s'_{i-n} of the data symbol s_{i-n} is now taken as the value of the x_{i-n} in the selected vector. Any vector P_i whose first component x_{i-n} differs from s'_{i-n} is then discarded by assigning to it a very high cost. From the remaining $\{P_i\}$, including that from which s_{i-n} was detected, are selected four vectors with the smallest cost $\{U_i\}$ and is designated as $\{Q_i\}$. The first component x_{i-n} of each of these four selected vectors $\{P_i\}$ is now omitted (without changing their cost). These four selected vectors $\{Q_i\}$ are now stored along with their associated costs $\{U_i\}$, where these costs are the same as those of the $\{P_i\}$ from which the $\{Q_i\}$ was derived.

The smallest of these costs is now subtracted from the four stored costs, so that the smallest cost becomes zero. This is performed in order to avoid an unacceptable increase in the value of the costs over a long message. It does not change the difference between the costs. The four selected vectors $\{Q_i\}$ are stored along with their costs $\{U_i\}$, and the detector is then ready for the next detection process, i.e. the detection of s_{i-n+1} on the receipt of r_{i+1}. In the case of two independently Rayleigh fading paths, Equation 7 can be rewritten as:

$$U_i = U_{i-1} + \left|r_i - x_{i-0}y_{i,0} - x_{i-1}y_{i,1}\right|^2 \quad \ldots (9)$$

5-POLE BESSEL FILTER USED FOR CHANNEL GENERATION

A Rayleigh fading transmission path is modelled as shown in Figure 5 where $q_1(t)$ and $q_2(t)$ are the two statistically independent Gaussian random waveforms with zero mean, and same variance and same power spectral density (which is assumed to be Gaussian). $n_1(t)$ and $n_2(t)$ are the Gaussian random numbers. Figure 3 illustrates the generation of $q_1(t)$ and $q_2(t)$ from $n_1(t)$ and $n_2(t)$. Figure 4 gives the block diagram of the generation of $q_i(t)$ from $n_i(t)$, where i is 1,2 respectively. Figure 5 illustrates the generation of $Q_g(t)$, the gth reflected Rayleigh fading path. Here in this work the total number of Rayleigh fading paths is two with 80% & 20% power distribution for the first and the second paths respectively i.e. in $Q_0(t)$ and $Q_1(t)$.

Consider the process $q_1(t)$. The power spectrum is given as,

$$|q_1(f)|^2 = exp\left[\frac{-f^2}{2f_{rms}^2}\right] \quad \ldots (10)$$

The cut-off frequency f_c is 3 dB (or half – power) power point and is given by the value of f in Equation 10 when,

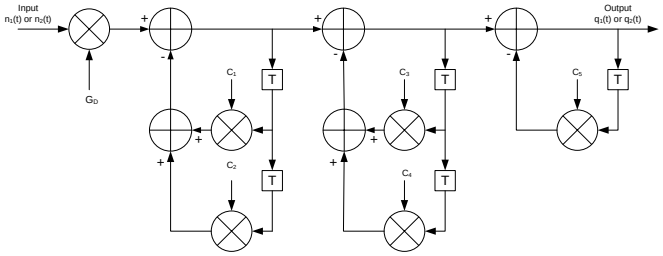

Fig. 3 5-pole Bessel Filter Used for Channel Generation

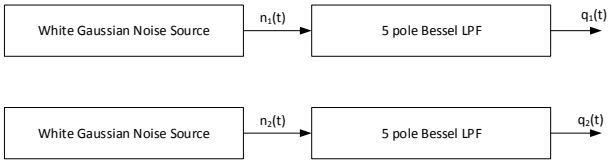

Fig. 4 Generation of $q_i(t)$ from $n_i(t)$

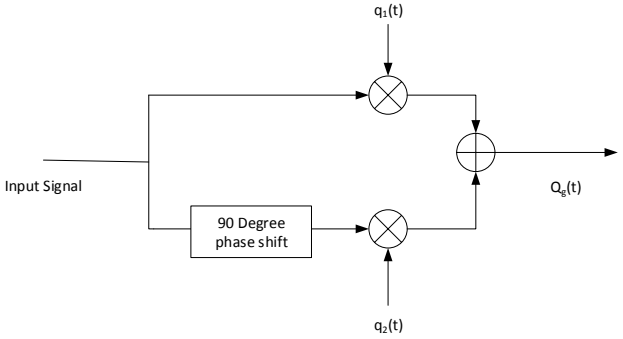

Fig. 5 Generation of $Q_g(t)$ from $q_i(t)$

$|q_1(f)|^2 = 0.4$ … (11)
(for variance = 0.4)
and
$|q_1(f)|^2 = 0.1$ … (12)
(for variance = 0.1)
Therefore,
$0.4 = exp\left[\frac{-f_c^2}{2f_{rms}^2}\right]$ … (13)
and
$0.1 = exp\left[\frac{-f_c^2}{2f_{rms}^2}\right]$ … (14)
Thus,
$f_c = 1.3537f_{rms}$ (for variance = 0.4) … (15)
$f_c = 2.1460f_{rms}$ (for variance = 0.1) … (16)
but,
$f_{rms} = \frac{f_{sp}}{2}$ … (17)
Therefore, from Equations 15, 16, and 17 we get
$f_c = 0.6768f_{sp}$ (For variance = 0.4) … (18)
and
$f_c = 1.0730f_{sp}$ (For variance = 0.1) … (19)
The frequency spread studied in this paper is,
$f_{sp} = 370\ Hz$ (For 80 km/h and a frequency of 5 GHz) … (20)
Thus the corresponding cut-off frequency will be
$f_c = 250.67\ Hz$ (for variance = 0.4) … (21)
And
$f_c = 397.41\ Hz$ (for variance = 0.1) … (22)
The transfer function in the s-plane of the 5-pole Bessel filter can be written as,
$H(s) = \frac{G_A}{\prod_{i=1}^{5}(s-p_i)}$ … (23)
where,
G_A = constant dependent on the cut-off frequency fc
s = Laplacian variable
p_i = s-plane poles of H(s)
When the 5-pole Bessel filter is normalized to cut-off (-3 dB) frequency of f_c = 1 Hz, the s-plane poles takes on the following values,
p_1 = -9.4394 … (24)
p_2, p_3 = -8.6764±j4.5108 … (25)
p_4, p_5 = -6.0173±j9.2434 … (26)
However, the cut-off frequency is not 1 Hz but is given by Equations 21 and 22. The s-plane poles corresponding to the required cut-off frequencies are next obtained by scaling the values in Equations 24, 25, and 26 by these values of f_c. These values are obtained as,
For variance = 0.4
p_1 = -2366.174 … (27)
p_2, p_3 = -2174.91±j1130.72 … (28)
p_4, p_5 = -1508.36±j2317.04 … (29)
For variance = 0.1
p_1 = -3751.31 … (30)
p_2, p_3 = -3448.09±j1792.64 … (31)
p_4, p_5 = -2391.34±j3673.42 … (32)
In order to implement the filter digitally, the s-plane poles must be transformed to the z-plane. In order to do this, **impulse invariant technique** is used, where the impulse response of the digital filter becomes sampled version of the impulse response of the analog filter, and the transfer function becomes,

$H(z) = \frac{G_D}{\prod_{i=1}^{5}(1-z_i z^{-1})}$ … (33)
where,
G_D = constant
z_i = z-plane poles

The mapping of the s-plane to the z-plane is done using transformation,

$z_i = exp(p_i T)$ … (34)

where T is the sampling interval in seconds. The sequence obtained at the output of this filter is equivalent to sequence obtained by sampling the waveform at the output of the original filter with the sampling interval of T seconds. The constant G_D at the input to the Bessel Filter (see Figure 3) is employed to change the variance of the $q_i(t)$ to their required values. The objective is to ensure that the total mean power input to the model is equal to the total mean power output. Thus, the total variance of all the $q_i(t)$'s together should be unity. Combined with the requirement the variance of all the $q_i(t)$'s should be equal, this implies that the space wave model under test, each $q_i(t)$ should have variance of 0.4 and 0.1 respectively thus making the total to unity (for the two paths taken together).

For example for the value of T = 1/1000000 (which is used in this work for 2 Mbps bit rate for QAM-4)

For variance = 0.4 the z_i are obtained as,

$z_1 = 0.9976$ … (35)

$z_2, z_3 = 0.9978 \pm j0.0011$ … (36)

$z_4, z_5 = 0.9995 \pm j0.0023$ … (37)

For variance = 0.1 the z_i are obtained as,

$z_1 = 0.9963$ … (38)

$z_2, z_3 = 0.9966 \pm j0.0018$ … (39)

$z_4, z_5 = 0.9976 \pm j0.0037$ … (40)

The 5-pole Bessel filter with the z-plane poles z_i (i = 1 to 5) is implemented as shown in Figure 3 where the tap gain coefficients are given by c_i (i = 1 to 5). This is a cascade of two-pole sections having complex conjugate poles (z_2 and z_3, z_4 and z_5) while the single 1-pole section has real pole (z_1).

It can be seen from Figure 3 that the transfer function of the first 2-pole section is given by,

$$T_1(z) = \frac{1}{1+c_1 z^{-1}+c_2 z^{-2}} \quad \text{… (41)}$$

$$T_1(z) = \frac{1}{1-(z_2+z_3)z^{-1}+(z_2 z_3)} \quad \text{… (42)}$$

$$T_1(z) = \frac{1}{(1-z_2 z^{-1})(1-z_3 z^{-1})} \quad \text{… (43)}$$

$$T_2(z) = \frac{1}{1+c_3 z^{-1}+c_4 z^{-2}} \quad \text{… (44)}$$

$$T_2(z) = \frac{1}{1-(z_4+z_5)z^{-1}+(z_4 z_5)} \quad \text{… (45)}$$

$$T_2(z) = \frac{1}{(1-z_4 z^{-1})(1-z_5 z^{-1})} \quad \text{… (46)}$$

$$T_3(z) = \frac{1}{1-z_1 z^{-1}} \quad \text{… (47)}$$

From Equations 41 and 43, 44 and 46, and 47

For variance = 0.4

$c_1 = -(z_2 + z_3) = -1.9956$

$c_2 = z_2 z_3 = 0.9956$

$c_3 = -(z_4 + z_5) = -1.9990$

$c_4 = z_4 z_5 = 0.9990$

$c_5 = -z_1 = -0.9976$

For variance = 0.1

$c_1 = -(z_2 + z_3) = -1.9932$

$c_2 = z_2 z_3 = 0.9932$

$c_3 = -(z_4 + z_5) = -1.9952$

$c_4 = z_4 z_5 = 0.9952$

$c_5 = -z_1 = -0.9963$

These values of the coefficient changes at run time depending upon the value of T, which is taken to be a constant at the start of the program.

Results and Discussions

The program is run in a number of channel configurations and the results so obtained are stored in a result file, each for a particular configuration. In all of the channel configurations, the value of the doppler spread in frequency is taken to be 370 Hz which corresponds to a mobile speed of 80 Kmph at 5 GHz frequency of transmission. The values of the sampling frequency for the digital Bessel filter varies from 1000000 samples/sec to 25000000 samples per second. The bit rate of the data communication corresponds to 2 Mbps and 50 Mbps respectively. The time taken by GPU for the transceiver signal processing for QAM-4 modulation scheme for different channel configurations are given in Table 1. From Table 1 it is evident that the total time for processing more than 300 MB data is only roughly around 676 ms which can be considered as real time. The number of bits transmitted in all the channel configurations is taken to be 46,724,547 bits in this work. The number of Rayleigh fading paths taken in this work is two with 80% and 20% power distribution for the first and the second paths respectively.

The BER vs SNR curves for the QAM-4 modulation scheme under different channel configurations is given in Figure 6. From the figure it can be observed that for low SNR, the BER for all the channel configurations is almost same, but for higher SNR, the BER for lower bit rate is lower than that of the higher bit rate. Under such conditions the 2 Mbps comes out to be much better than 50 Mbps at higher SNRs. Moreover, as can be seen in the Figure 6 that at higher SNRs the BER of system having the bit rate ranging from 40 Mbps till 50 Mbps is almost neck to neck. Hence, over the 40 Mbps speed the BER of the system is not much different for higher bit rate upto 50 Mbps. Moreover, as can be observed from the figure, the performance in SNR for 20 Mbps speed is only about 10 dB lower than that at 40 Mbps speed for the same BER (say at 1.00E-04).

For the same BER, the SNR required for the system with higher bit rate is higher than that of the system with lower bit rate. The 20 Mbps system has SNR of about 55 dB for a bit error rate of 1.00E-04. The 50 Mbps system has the SNR of about 60 dB for a bit error rate of say 1.00E-04. Hence, for higher bit rate, the transmitted power has to be increased to meet the same performance by a system with lower bit rate.

Table-1 The Profiler Statistics For NVIDIA GeForce GTX 1050 Ti GPU

Feature	Value
Total Host to Device Memory Transfer	373.2 MB
Host to Device Memory Transfer Time	78.46 ms
Total Device to Host Memory Transfer	367.5 MB
Device to Host Memory Transfer Time	202.048 µs
GPU Time for Baseband Processes	676.67 ms
GPU Occupancy (Compute Utilization)	90.2 %
Threads per Block	512
Blocks per Grid	147
CUDA Cores	768
Processing Speed (FLOPS)	2.24 Tera FLOPS

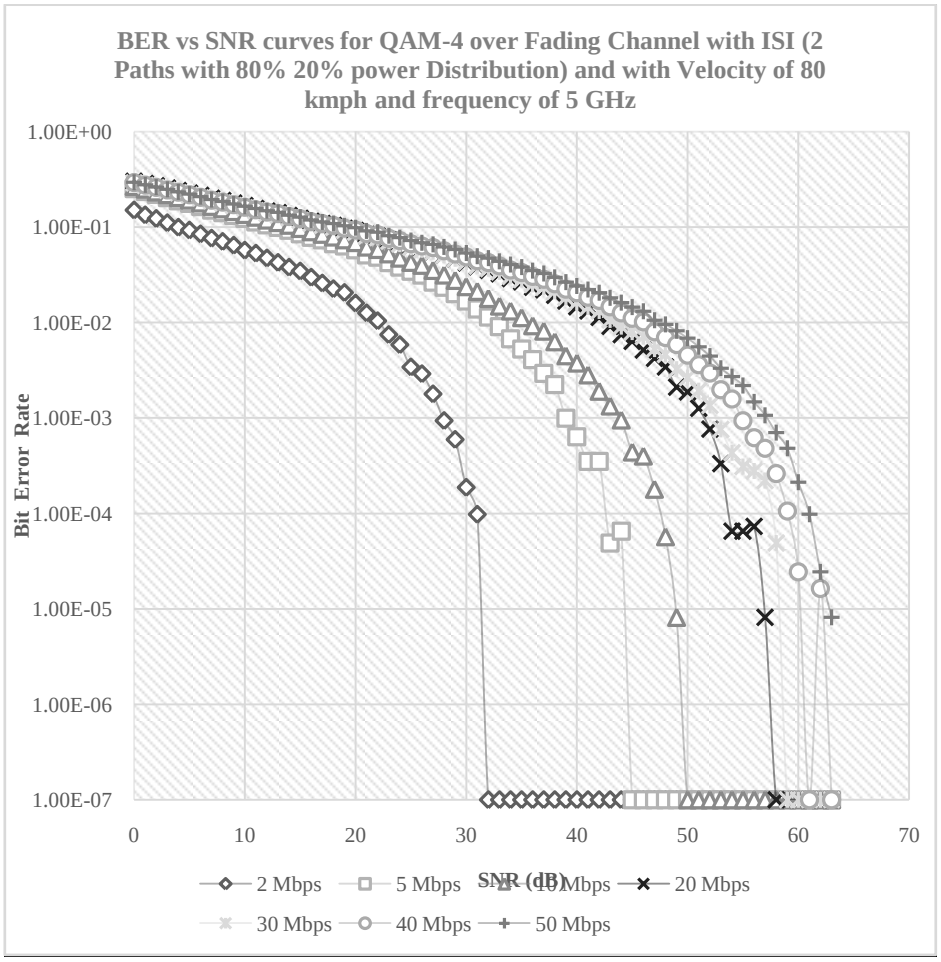

Fig. 6 The BER vs SNR curves for QAM-4 for different Bit Rates

CONCLUSIONS

The transceiver for the QAM-4 Modulation scheme is tested using CUDA-C++ programming language on an NVIDIA GPU. The detection scheme used at the receiver is Near-maximum-likelihood detection. This program is run on a Personal Computer having an 8th generation core i3 processor. The NMLD scheme and the 5-pole Bessel filter used for channel generation is discussed in detail. Hence, by changing a few parameters different channel configurations can be simulated. This can be done at run time by some clever programming of the GPU. The results in BER vs SNR curves for QAM-4 modulation scheme suggest that for higher SNRs, the higher bit rate system gives poor results as compared to lower bit rate. If the receiver is designed to work in these severe conditions, and works satisfactorily, it can work perfectly well in less severe conditions. Moreover, since the processing is done almost real time, the GPU can be used at the baseband section of an SDR.

REFERENCES

[1]. N. Boudriga, "Tutorial 4: Security of Mobile Communications", 2007 IEEE International Conference on Signal Processing and Communications (ICSPC 2007), 24-27 November 2007, Dubai, United Arab Emirates, pp. 1i-1ii.

[2]. J. Z.Sun and J.Sauvola, "On Fundamental Concept of Mobility for Mobile Communications", The 13th IEEE International Symposium on Personal, Indoor and Mobile Radio Communications, 2002, pp. 799-803.

[3]. K. Tachikawa, "A Perspective on the Evolution of Mobile Communications", IEEE Communications Magazine, Vol. 41, Issue 10, 2003, pp. 66-73.

[4]. T. Otsu, I. Okajima, N. Umeda, and Y. Yamao, "Network Architecture for Mobile Communications Systems Beyond IMT-2000", IEEE Personal Communications Magazine, Vol. 8, Issue 5, 2001, pp. 31-37.

[5]. T. Ohseki, N. Fuke, H. Ishikawa, and Y. Takeuchi, "Multihop Mobile Communications System Adopting Fixed Relay Stations and its Time Slot Allocation Schemes", 2006 IEEE 17th International Symposium on Personal, Indoor and Mobile Radio Communications, 2006, pp. 1-5.

[6]. D. Raychaudhuri and N. B. Mandayam, "Frontiers of Wireless and Mobile Communications", Proceedings of IEEE, Vol. 100, Issue 4, pp. 824-840.

[7]. M. Israil and M. S. Beg, "Mitigation of ISI for next generation wireless channels in outdoor vehicular environments", International Journal of Electronics, Communication & Computer engineering, France, Vol. 1, No. 3, 2009, pp. 150-155 (ISSN 2073-0543).

[8]. R. Muzammil; M. Salim Beg; M. M. Jamali; and M. W. Majid, "Design and testing of a Software Defined Radio based transceiver on a Graphics Processing Unit", 2012 Conference Record of the Forty Sixth Asilomar Conference on Signals, Systems and Computers (ASILOMAR), 2012, pp. 1107-1110.

[9]. C. H. Dick, "Design and Implementation of High-Performance FPGA Signal Processing Data paths for Software Defined Radios", VME and Critical Systems, August 2001 (VME 1664).

[10]. O. Zlydareva and C. Sacchi,; "Multi-Standard WIMAX/UMTS System Framework Based on SDR", Aerospace Conference, 2008 IEEE, pp.1-13

Rehan Muzammil received the B.Sc. Engg. (Electronics) Degree in 1990, M.Sc. Engg. (Electronics) degree in 1996, and PhD degree in Electronics Engineering in 2015, from Aligarh Muslim University. He has also worked in BHEL, India and HCL Perot System, India. Recently he is working as an Assistant Professor in the Department of Electronics Engineering, Aligarh Muslim University, India since 2017. His research areas are SDR, DSP, Digital Communications, and Digital System Design.